Terbit online pada laman web jurnal: **https://journal.isas.or.id/index.php/JAMERE**

JOURNAL OF APPLIED MECHANICAL ENGINEERING AND RENEWABLE ENERGY (JAMERE)

Vol. 4 No. 2 Agustus 2024 67-75 ISSN: 2775-1031

Airflow Velocity Measurement Of Turbular Test Section Based On RPM Setting Configuration In Open Circuit Subsonic Wind Tunnel

Nanda Syifa Fauziah Rahmani[1], Sugianto[2], Deden Masruri[3]
[1]Jurusan Teknik Mesin , Politeknik Negeri Bandung
[1]nanda.syifa.aer21@polban.ac.id, [2]sugianto@polban.ac.id*, [3]dedenmasruri@polban.ac.id

Abstract

Speed measurements in the test section based on the RPM setting configuration of the open-type subsonic wind tunnel with a turbular test section to obtain the properties of the airflow in the test section based on the RPM setting configuration in the open-type subsonic wind tunnel. The simulation process is carried out using software Computational Fluid Dynamics (CFD) , ANSYS Fluent. The simulation process is carried out by the method Moving Reference Frame (MRF) that the fluid phenomenon is moved to move the fan in the wind tunnel to obtain airflow properties in the turbular test section, open-type subsonic wind tunnel. In the testing process, airflow velocity measurements were carried out in the turbular test section of the open-type subsonic wind tunnel using an air velocity measuring instrument, namely anemometer and hotwire. The software Computer Aided Design (CAD), Solidworks, serves to create the geometry of the open-type subsonic wind tunnel and has a turbular test section inspired by the Didacta Italia PN21 D open-type subsonic wind tunnel. The properties that occur in the test section based on the configuration of the RPM setting in the open-type subsonic wind tunnel turbular test section are expected to achieve results to obtain the value of the velocity distribution, pressure distribution and turbulence intensity value so that it is useful and supports the operation and testing process to be carried out in an open-type subsonic wind tunnel with a turbular test section.

Keywords: wind tunnel, fluid computation, fan simulation, moving reference frame, test section.

1. Introduction

The use of wind tunnels today has clear uses and wide applications in various scientific fields, especially in the field of transportation and aerodynamics. When wind tunnels first appeared, aerodynamicists began to understand the factors that control airflow velocity in wind tunnels. Wind tunnels have the role and ability to recognize the aerodynamic forces and moments that act on the conditions inside the wind tunnel and the objects in it [1].

In general, the fan in the wind tunnel is driven by a motor to move the fan with RPM settings adjusted as needed. The speed of the airflow produced by the fan is very influential because the RPM setting on the motor to move the fan in accordance with the RPM is set [2][3]. This requires a maintenance process as well as a periodic measurement process to keep the wind tunnel working optimally, to achieve ideal test conditions.

This study will conduct a speed measurement that flies one setting on the blade angle on the wind tunnel fan and four variations of rotational speed on the fan with RPM settings, at RPM 500, RPM 750, RPN 1000, and RPM 1250 airflow to obtain airflow properties in the turbular test section, in an open-type subsonic wind tunnel with variations in fan rotational speed in the wind tunnel. In the test section of the wind tunnel using an analytical approach with CFD (Computational Fluid Dynamics) simulation with the moving reference frame (MRF) method and testing with airflow velocity measurements in the wind tunnel to measure the speed of the turbular test section based on the RPM configuration in an open-type subsonic wind tunnel inspired by the Didacta Italia PN21 D wind tunnel.

Thus, this study will obtain the value of the velocity distribution in the airflow in the wind tunnel test section, the value of the pressure distribution in the airflow in the wind tunnel test section and the value of the turbulence intensity in the airflow in the wind tunnel test section. By obtaining these data, steps to facilitate the operation of the wind tunnel are needed by setting the RPM in the wind tunnel.

2. Research Methods

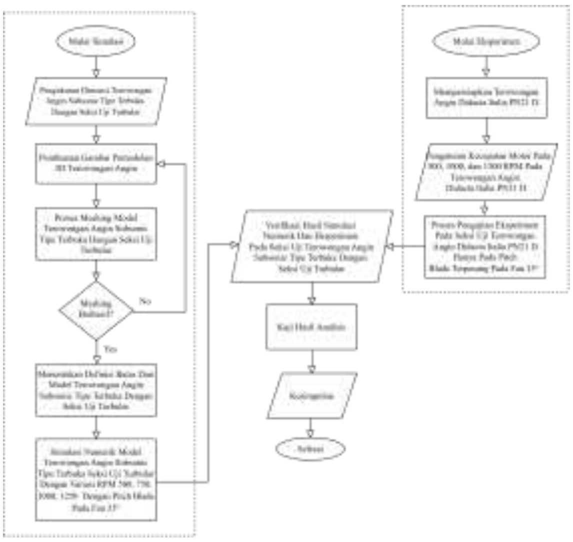

Figure. 1 Flow chart

2.1 Measurement of Wind Tunnel Dimensions

Figure. 2 Didacta Italia PN21 D Wind Tunnel

Take measurements of the wind tunnel that meet the needs in the design process for reference to the 3D model of the wind tunnel. The subsonic wind tunnel is open type and has a turbular test section inspired by Didacta Italia PN21 D. In the process of measuring dimensions in the wind tunnel using measuring instruments such as a meter, vernier caliper, ruler.

2.2 Design of the 3D Wind Tunnel Model

In the process of designing a 3D wind tunnel model using CAD (Computer Aided Design) software, namely Solidworks. In the process of making 3D model by making open-type subsonic wind tunnel parts by drawing parts of the wind tunnel that refer to and are inspired by the results of dimensional measurements on the Didacta Italia PN21 D wind tunnel that have been carried out. The process of making wind tunnel geometry includes parts, bellmouth / contraction cone, test section, diffuser, blade of the fan, and hub on the fan.

2.3 Wind Tunnel Model Meshing Process

The meshing process is carried out using ANSYS software. The meshing process aims to divide the plane into small elements that can be studied in numerical simulations, the method used in this simulation is the multi-block method where the geometry meshes individually based on its volume. This method is also used to provide different mesh variants at each geometry level as required and as a solution for complex geometry parts such as fans. Different mesh types are selected based on their respective geometries and customized to the shape of the geometry as needed [2].

2.4 Determination of Wind Tunnel Boundary Definitions

The process of determining the definition of boundary physics in an open-type subsonic wind tunnel. There is a predetermined domain, namely the moving fluid domain and the stationery fluid domain, at the boundary type is the determination of input data which is the boundary of the flow modeling area in the fluid. At the boundary inlet with the boundary type, namely pressure inlet, input pressure data is 1 bar (mean sea level). Available in Table. 1

Table. 1 Boundary Condition Windtunnel

Domain	Boundaries	Type
Moving Fluid	Boundary - Casing Fan 2	Wall
	Boundary - Default Interior 012 Moving Fluid	Interface
	Boundary - Fan 35 Degree	Wall
Stationery Fluid	Boundary - Bellmouth	Wall
	Boundary - Casing Fan 1	Wall
	Boundary - Default Interior 012 Stationery Fluid	Interface
	Boundary - Inlet	Pressyre Inlet
	Boundary - Junction Pipe	Wall
	Boundary - Outlet	Pressure Outlet
	Boundary – Test Section	Wall

2.5 Wind Tunnel Testing Process

The testing process was carried out to obtain the airflow velocity distribution in the test section at a pitch angle on the blade attached (35°) to the fan blade shaft in the Didacta Italia PN21 D wind tunnel. In the Didacta Italia PN21 D wind tunnel using four RPM settings at RPM 500, RPM 750, RPM 1000, RPM 1250 on the fan drive motor in the PN21 D wind tunnel and setting four RPM variations are involved in the simulation process.

2.6 Measurement of Velocity Distribution Using an Anemometer

The use of an anemometer to measure the velocity distribution of airflow in the test section of the PN21 D wind tunnel is carried out at several points along the y-axis of the test section. These points include positions near the bottom wall, the middle of the test section, and near the top wall. The wind tunnel's RPM settings are adjusted to 500 RPM, 750 RPM, 1000 RPM, and 1250 RPM. This is done to measure the velocity distribution across the cross-section of the wind tunnel test section.

2.7 Measurement of Velocity Distribution Using a Hotwire

Measurement of Airflow Velocity Distribution in the test section of the PN21 D wind tunnel is conducted to serve as a comparison and validation of the hotwire measurements. This process involves setting the RPM at 500 RPM, 750 RPM, 1000 RPM, and 1250 RPM. The hotwire is positioned at the same three points as the anemometer, aligned with their respective positions near the bottom wall, middle of the test section, and near the top wall.

2.8 Conclusion

The process of drawing conclusions gets the results of the testing process in the form of airflow velocity distribution values in the wind tunnel test section. The results of the simulation process will produce properties that occur in the airflow in the wind tunnel test section. The airflow properties are the airflow velocity distribution value, the airflow pressure distribution and the turbulence intensity value in the airflow.

3. Results and Discussion

3.1 Wind Tunnel Modeling Results

Measurement results of the wind tunnel geometry inspired by the open-type subsonic wind tunnel Didacta Italia PN21 D, featuring a tubular test section. The dimensional results are presented in Table. 2.

Table. 2 Measurement Results of Wind Tunnel Modeling

Part	Dimension	Information
Bellmouth	Length : 993 mm	
	Width : -	
	Thickness : 9,55 mm	
	Diameter : 300 mm	Rear Diameter
	Diameter : 920 mm	Front Diameter
Test Section	Length : 2000 mm	
	Width : -	
	Thickness : 7 mm	
	Diameter : 300 mm	
Drive Section	Length : 300 mm	
	Width : -	
	Thickness : 7 mm	
	Diameter : 300 mm	
Hub Assembly	Length : -	
	Width : -	
	Thickness : 40 mm	
	Diameter : 140 mm	
Blade	Length : 53,43 mm	
	Width : 76 mm	
	Thickness : -	
	Diameter : 30 mm	Hub Blade

In creating the wind tunnel geometry using CAD software such as SolidWorks, the process typically starts with sketching, followed by creating individual parts and then assembling them. In the fan assembly, detailed drawings show fasteners attached to the shaft, connecting the hub assembly. This approach ensures a comprehensive design of the wind tunnel model, as illustrated in the figure.

Figure. 3 Results of 3D Wind Tunnel Model Design

Figure. 4 Results of 3D Wind Tunnel Model Design

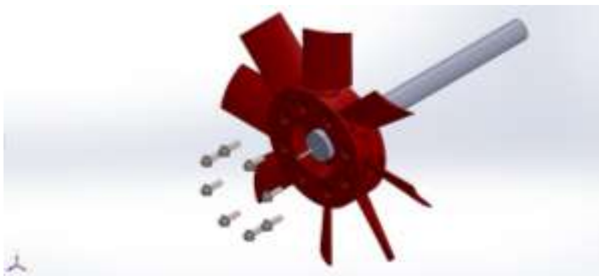

Figure. 5 3D Model of Fan Assembly in the Wind Tunnel

3.2 Wind Tunnel Modeling Meshing Results

In the process of meshing the open-type subsonic wind tunnel model, the workflow involves importing the geometry designed in CAD software into CFD software using an IGS file format. Therefore, it is necessary to simplify the geometry shape, particularly in the main components of the wind tunnel, without involving the detailed modeling as done in CAD software. This simplification may lead to a new definition of geometry. In the bellmouth, test section, and diffuser sections, hexahedral, tetrahedral, and triangular meshing techniques are utilized. Figure 6 illustrates the overall meshing results, while Figures 7 to 9 provide detailed views of the meshing outcomes of the wind tunnel.

Figure. 6 Results of Wind Tunnel Meshing

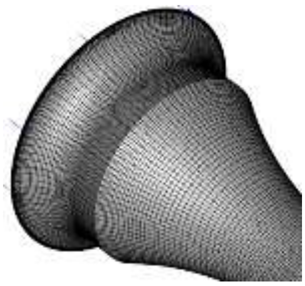

Figure. 7 Results of Hexahedral Meshing on Bellmouth

Figure. 8 Results of Hexahedral and Tetrahedral Meshing

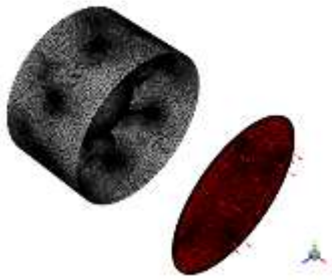

Figure. 9 Results of Tetrahedral Meshing on the Fan Casing

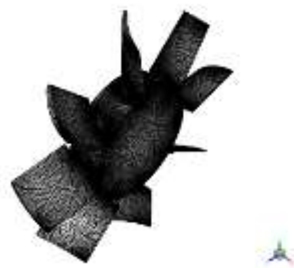

Figure. 10 Results of Tetrahedral Meshing on the Fan

3.2.1 Results of Determining Boundary Definitions

The process of determining the definition of boundaries and conditions that occur in the simulation is listed in the table.

Table. 3 Boundary Conditions

Boundary Conditions	Model	Information
Domain Moving Fluid	Cell	
Domain Stationery Fluid	Cell	
Model Viscous	k-epsilon	
Model Turbulent	Intensity and Hydraulic Diameter	Intensitas Turbulensi : 5%
Inlet	Pressure Inlet	Pressure Gate (P_g) : 0
Outlet	Pressure Outlet	Diameter hidrolik : Bellmouth : 920 mm Test Section : 300 mm Casing Fan : 300 mm
Blade	(Moving Reference Frame) MRF	RPM 500, RPM 750, RPM 1000, RPM 1250
Blade	Wall	V : 0

3.2.2 Wall Y Plus Value Simulation Results

Figure 11, it shows the wall y plus values along the open-type subsonic wind tunnel, indicating the mesh quality near the walls improves with smaller mesh sizes. In the bellmouth section, an optimal wall y plus value ranges from 0 to 2, while in the test section, it ranges from 4 to 6. A significant difference occurs in the fan area where the highest wall y plus values are observed. This discrepancy is due to meshing adjustments that accommodate the complexity level of the geometry, particularly in the fan region.

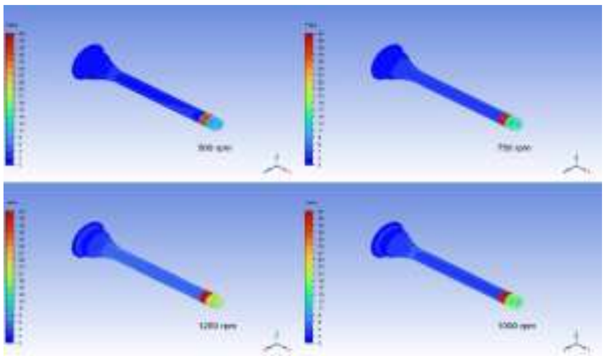

Figure. 11 Wall Y Plus Value in Wind Tunnels

3.3 Simulation Results of Air Flow Visualization in an Open Circuit Subsonic Wind Tunnel

The simulation results for the open-type subsonic wind tunnel with a tubular test section were conducted at RPM 500, RPM 750, RPM 1000, and RPM 1250. As shown in Figure IV.5, the visualization illustrates varying airflow velocities in different sections and depicts the direction of airflow. As the airflow approaches the fan, its pattern becomes conical. When the fan rotates, the airflow around the fan becomes turbulent, differing from the airflow in the bellmouth and along the test section before reaching the fan. The wind speed increases after passing through the fan due to the fan's rotation. Figure 12 shows the visualization of streamlines airflow in the diffuser and fan regions.

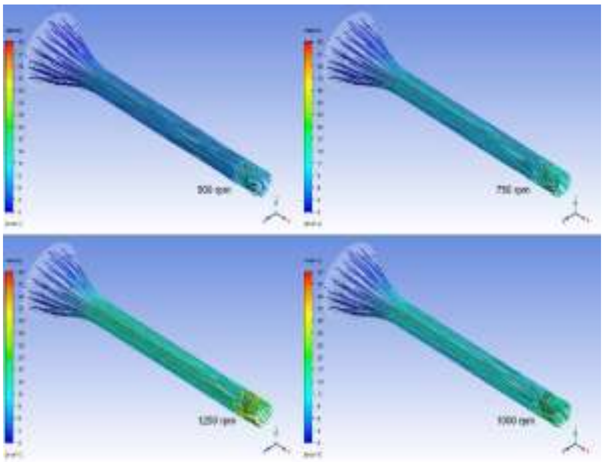

Figure. 12 Wind Tunnel Air Flow (Streamline) Visualization

3.4 Simulation Results of Air Flow Velocity Distribution in an Open Circuit Subsonic Wind Tunnel

The airflow velocity simulation results for the open-type subsonic wind tunnel with a tubular test section involve four RPM configurations (RPM 500, RPM 750, RPM 1000, and RPM 1250). Figure 13 shows the airflow velocity in the wind tunnel using cross-sections along the X, Y, and Z axes. It can be observed that the bellmouth section has a lower velocity compared to other parts of the wind tunnel. The airflow velocity at the inlet of the bellmouth for all four RPM variations tends to be low, ranging from 0 m/s to 3 m/s. As the airflow progresses towards the test section, the velocity increases at each RPM. In the test section, the velocity reaches 6 m/s at RPM 500, 8 m/s at RPM 750, 10 m/s at RPM 1000, and 13 m/s at RPM 1250.

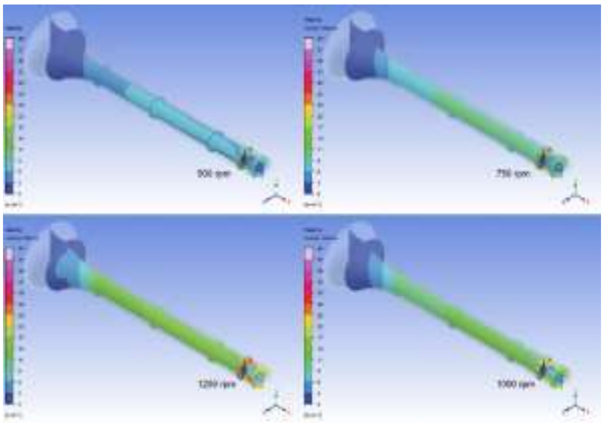

Figure. 13 Speed Distribution Values in Wind Tunnels

3.5 Simulation Results of Pressure Distribution in an Open Circuit Subsonic Wind Tunnel

The results of pressure distribution in an open-type subsonic wind tunnel with a turbular test section involve 4 RPM variations, namely at (RPM 500, RPM 750, RPM 1000, RPM 1250). Can be seen in Fig. 14 shows the pressure distribution that occurs, the results show the lowest pressure distribution value found in the wind tunnel test section. The pressure distribution along the wind tunnel at 4 RPM variations is 1 bar.

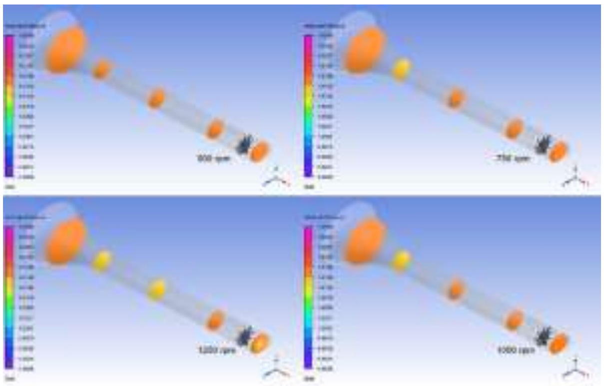

Figure. 14 Pressure Distribution Values in Wind Tunnels

3.6 Simulation Results of Turbulence Intensity in an Open Type Subsonic Wind Tunnel

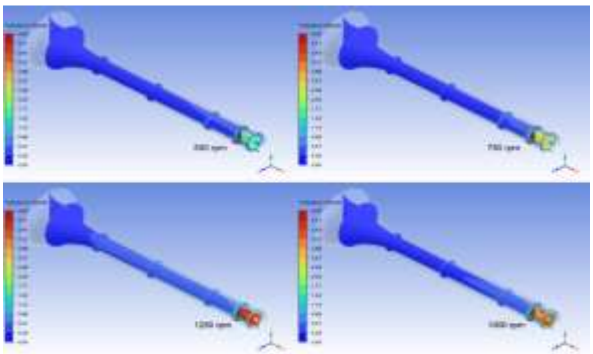

Figure. 15 Turbulence Intensity Values in Wind Tunnels

The wind tunnel is designed to produce high velocities with laminar airflow conditions. Additionally, the test section of the wind tunnel must have low turbulence intensity. The simulation results for turbulence intensity in the open-type subsonic wind tunnel with a tubular test section show values below 5% across the four RPM settings. This is illustrated in Figure 15, which shows the turbulence intensity in the wind tunnel with an isometric view on the (X, Y, Z) plane.

3.7 Air Flow Velocity Distribution Curve in an Open Type Subsonic Wind Tunnel

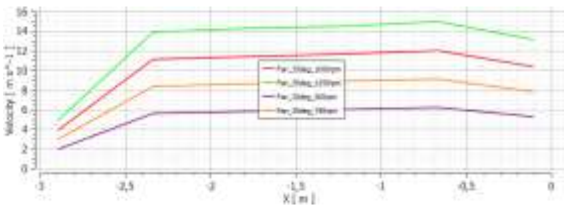

Figure. 16 Air Flow Velocity Profile in a Wind Tunnel

In Figure 13, the contour of airflow velocity distribution in the wind tunnel is shown with four RPM variations and a fan angle of 35 degrees. Figure 16 displays the velocity distribution profile of the airflow in the wind tunnel, comparing the results of the airflow velocity distribution simulation with the wind tunnel's dimensional coordinates. The curve results show that at RPM 1250, the highest velocity in the test section reaches 14 m/s. At RPM 1000, the velocity in the test section is 11 m/s. At RPM 750, the velocity in the test section is 8.5 m/s, and at RPM 500, the velocity distribution in the test section is 5.5 m/s. As the RPM increases, the airflow velocity distribution produced also increases.

3.8 Air Flow Pressure Distribution Curve in an Open Circuit Subsonic Wind Tunnel

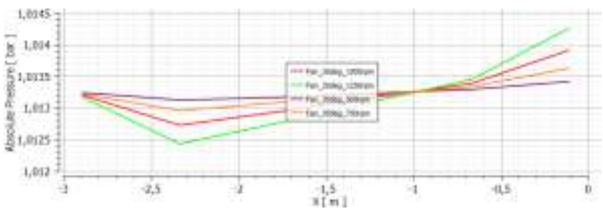

Figure. 17 Pressure Distribution Profile in Wind Tunnel

In Figure 17, the pressure distribution profile of the airflow in the wind tunnel is shown with four RPM variations and a fan blade angle set at 35 degrees. Figure 14 displays the pressure distribution contour in the wind tunnel. It can be seen that Figure 17 shows the pressure distribution values, particularly in the test section of the wind tunnel, where the highest pressure is observed at RPM 500. At RPM 1250, despite having the highest velocity, the pressure distribution is the lowest. This relates to the theoretical foundation discussed in Chapter 2 concerning the continuity equation for incompressible fluids, which have a constant fluid density. Therefore, based on the results of the airflow velocity distribution and pressure distribution along the wind tunnel, it can be concluded that these two variables are inversely related.

3.9 Wind Tunnel Experiment Results

3.9.1 Results of measuring air speed values against RPM using an anemometer

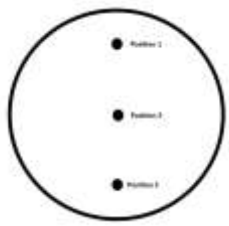

Figure. 18 Air Flow Velocity Measurement Position on Test Section Cross-Section

Air velocity measurements during the wind tunnel testing were conducted using an anemometer in the test section. Measurements were taken at four RPM variations: RPM 500, RPM 750, RPM 1000, and RPM 1250, with the testing process referencing anemometer positions as shown in Figure 18. The purpose of measuring airflow velocity at these three points is to determine the velocity distribution across the cross-sectional area of the wind tunnel test section. Below are the results of the airflow velocity measurements using an anemometer in the test section at the three anemometer measurement positions.

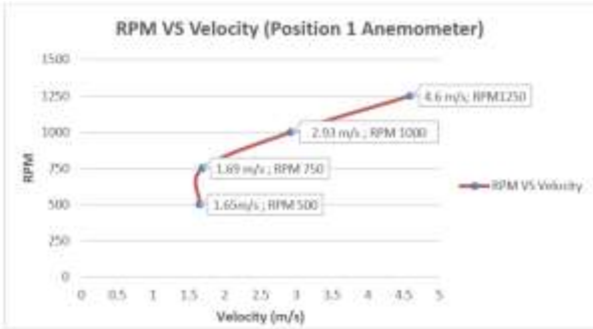

Gambar. 19 Measurement Results Using Anemometer Position 1

In Figure 19, the measurement results using an anemometer at the first position, 5 cm from the wind tunnel wall along the positive y-axis, close to the test section wall, are shown. The airflow velocity measurements obtained are 1.65 m/s at RPM 500, 1.69 m/s at RPM 750, 2.93 m/s at RPM 1000, and 4.6 m/s at RPM 1250.

The measurements at the second anemometer position are shown in Figure 20, where the anemometer is 15 cm from the test section wall along the positive y-axis, positioned at the center of the x-axis or the midpoint of the circle. The results obtained are 1.63 m/s at RPM 500, 1.68 m/s at RPM 750, 2.92 m/s at RPM 1000, and 4.57 m/s at RPM 1250.

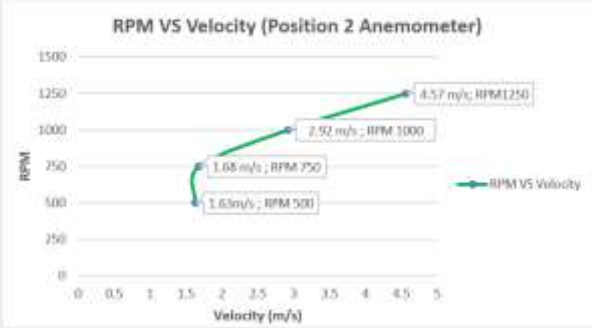

Figure. 20 Measurement Results Using Anemometer Position 2

In the third position in the measurement of air flow velocity in the wind tunnel test section using an anemometer placed at a distance of 10 cm towards the negative y axis adjacent to the wind tunnel wall. Can be seen the measurement results in the third position of the anemometer in Fig. 21 shows that at RPM 500 the airflow velocity result is 1.58 m / s, at RPM 750 it is 1.68 m / s, at RPM 1000 it has an airflow velocity value of 2.85 m / s and at RPM 1250 it has a velocity value of 4.56 m / s. The results of the three measurement positions using an anemometer can be seen in Figure 21. The results of the three measurement positions using an anemometer are relatively the same in each of the four RPM variations, there is an increase in the value of air velocity as the RPM setting changes. The greater the RPM setting, the greater the value of the resulting air velocity.

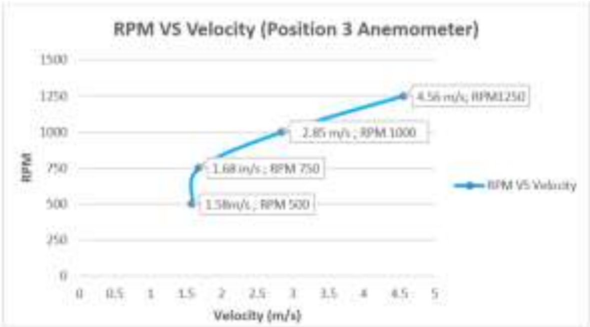

Figure. 21 Measurement Results Using Anemometer Position 3

3.2.1 Results of measuring air speed values against RPM using Hotwire

Figure. 22 Testing Positions Using Hotwire

The results of measuring the value of air velocity against RPM using a hotwire were carried out on the test section with three hotwire measurement positions during the test. In Fig. 22 shows the three positions in the direction of the y-axis, in the first position shows the position of the hotwire 5 cm from the wind tunnel wall, namely on the positive y-axis adjacent to the wall of the wind tunnel test section. In the second position, 15 cm away from the wall of the wind tunnel test section from the positive y-axis, coinciding with the middle position of the x-growth or at the center of the circle point. And in the third position, which is 10 cm away towards the negative y axis adjacent to the wind tunnel wall.

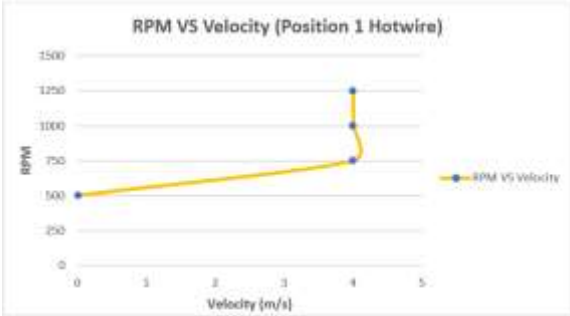

Figure. 23 Measurement Results Using Hotwire Position 1

In Figure 23, the results of airflow velocity measurements using a hotwire at the first position, located 5 cm from the test section wall along the positive y-axis, show that at RPM 500, the airflow velocity was 0 m/s, indicating very low airflow conditions that were undetectable by the hotwire. At RPM 750, the airflow velocity increased to 4 m/s, indicating an increase in airflow velocity at this RPM setting. At RPM 1000, the airflow velocity remained constant at 4 m/s, which was consistent with the results at RPM 750 and RPM 1250. The measurement process was conducted at the second position using a hotwire in the wind tunnel test section, precisely at the center point of the test section circle, located 15 cm along the positive y-axis. The velocity measurement results at the second hotwire position can be seen in Figure 24. At RPM 500, the airflow velocity was 0 m/s, similar to the first hotwire position. At RPM 750, the airflow velocity was 4 m/s, consistent with the results at RPM 1000 and RPM 1250.

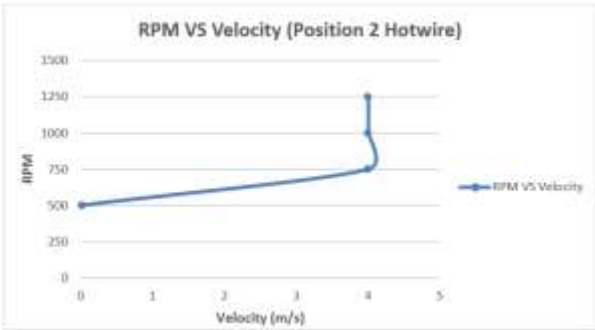

Figure. 24 Measurement Results Using Hotwire Position 2

During the testing, the placement of the hotwire at the third position resulted in airflow velocity measurements. At RPM 500, the airflow velocity was recorded as 0 m/s, which remained constant across all three positions. The airflow velocity at RPM 500 was very low, so low that it could not be detected by the hotwire. At RPM 750, the velocity increased to 4 m/s from its previous 0 m/s. At RPM 1000, the airflow velocity decreased to 3 m/s despite an increase in RPM, and the same result was observed at RPM 1250, where the airflow velocity remained constant at 3 m/s, similar to RPM 1000. Figure. 25 illustrates these findings.

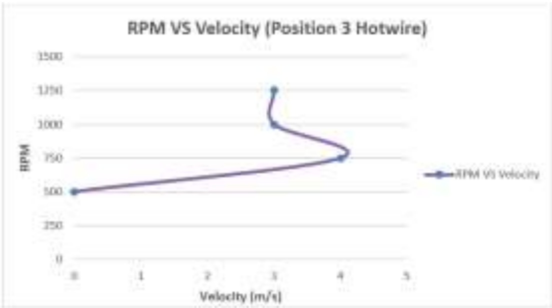

Figure. 25 Measurement Results Using Hotwire Position 3

Table. 4 Results of Airflow Velocity in Test Section

RPM	Anemometer	Hotwire	Simulation
500	0 m/s	1,63 m/s	5,5 m/s
750	4 m/s	1,68 m/s	8,5 m/s
1000	4 m/s	2,92 m/s	11 m/s
1250	4 m/s	4,57 m/s	14 m/s

4. Conclusion

1. With the difference in RPM can provide an increase in the value of airflow velocity at setting the blade angle in the wind tunnel 35 degrees and setting the RPM at RPM 500, RPM 750, RPM 1000, RPM 1250.
2. The simulation process results in an increase in the airflow velocity value in the wind tunnel test section as the RPM setting increases. The result of airflow velocity in the wind tunnel test section at RPM 500 is 5.5 m/s, RPM 750 is 8.5 m/s, RPM 1000 is 11 m/s and RPM 1250 is 14 m/s.
3. The tubulence intensity value generated through the simulation process is 4% in the wind tunnel.
4. The pressure distribution value produced by the simulation process shows a decrease as the RPM increases due to the increase in air flow velocity so that the pressure decreases. The pressure distribution results generated from the simulation process are at RPM 500 of 1.0142 bar, RPM 750 of 1.0117 bar, RPM 1000 of 1.0117 bar and RPM 1250 of 1.0130 bar.

Reference List

[1] D. D. B. and W. R. Corliss (2021). *Wind Tunnels of NASA*. NASA Official. [Online]. Available: https://www.grc.nasa.gov/WWW/k12/WindTunnel/history.html. [Accessed 13 May 2021]

[2] M. F. H. Freindsisco Xaverius, 2022. Rancang Bangun Terowongan Angin Kecepatan Rendah Tipe Terbuka Sederhana Dengan Smoke Generator Sebagai Visualisasi Aliran Udara Untuk Alat Praktikum. J. Kaji. Tek. Mesin, vol. 7, no. 2, pp. 63–72.

[3] R. Abdillah, Yopa, E. Prawatya, and R. A. Wicaksono (2021). Optimasi Desain Terowongan Angin Tipe Sirkuit Terbuka Menggunakan Metode Computer-Aided Simulation And Taguchi (CAST). vol. 2, no. 2, pp. 184–191.

[4] M. J. Sidiq, Politeknik Negeri Bandung, 2014. Simulasi Numerik Aliran Udara Internal di Terowongan Angin Loop Terbuka Kecepatan Rendah. Bandung, Indonesia.

[5] W. H. Rae and A. Pope., 1999. Low-Speed Wind Tunnel Testing. 3rd ed. London: A Wiley-Interscience publication.

[6] T. M. I. Hakim, 2015. Evaluasi Perancangan Terowongan Angin LS-LST Dengan Simulasi Numerik. Litbangyasa Teknol. Pada Pesawat Terbang, Roket, vol. 5,pp.101–106. Available:http://karya.brin.go.id/id/eprint/11046/%0Ahttp://karya.brin.go.id/id/eprint/11046/1/BungaRampai_Teuku_Pustekbang_2015.pdf

[7] D. Rhakasywi and A. Suwandi, Universitas Pancasila, 2017. Pengembangan Terowongan Angin Rangkaian Terbuka Dengan Sistem PIV (Particle Image Velocimetry).

[8] H. N. Firmansyah, P. Wirardi, R. F. Naryanto, and K. Karnowo, 2023. Simulasi 3D dan Studi Eksperimental Aliran Udara pada Variasi Geometri Menggunakan Wind Tunnel. J. Rekayasa Mesin, vol. 18, no. 3, p. 395. Available: doi :10.32497/jrm.v18i3.4973.

[9] Anonim. Didacta Italia S.R.L, Developmentaid. Available: https://www.developmentaid.org/organizations/view/6480/didacta-italia-srl

[10] J. Niulai and N. D. Muskitta, 2022. Pengaruh Bentuk Benda Uji Terhadap Pola Aliran Angin Di Ruang Uji Wind Tunnel. LPPM Politek. Saint Paul Sorong, vol. 7, no. 1, pp. 37–46.

[11] A. Ageng Riyadi. Pembuatan dan Pengujian Terowongan Angin Kecepatan Rendah Tipe Terbuka (Open Circuit Low Speed Wind Tunnel).

[12] A. T. Teseletso, M. Namoshe, N. Subaschandar, and S. Kutua, 2015. Design of an Open-circuit Subsonic Wind Tunnel For Educational Purpose. Botswana Inst. Eng. 14th Bienn. Conf., no. outubro.

[13] M. Singh, N. Singh, and S. K. Yadav, 2013. Review of Design and Construction of An Open Circuit Low Speed Wind Tunnel. Glob. J. Res. Eng., vol. 13, no. 5, pp. 1–22.

[14] N. Paul David Rey, Amiral Aziz, Dudung Hermawan, Muhammad Fahmi, 2020. Desain Dan Rancang Bangun Alat Uji Open Circuit Wind Tunnel

Tipe Subsonic. KOCENIN Ser. Konf., vol. 1, no. 1, pp. 1–11. Available:https://www.bing.com/ck/a?!&&p=1f95cfc671a920d0JmltdHM9MTcwMzM3NjAwMCZpZ3VpZD0zNDk2OGI2Yy1kZmYwLTYzMjMtMjRlMS05OTdiZGU1YzYyNTcmaW5zaWQ9NTE4MA&ptn=3&ver=2&hsh=3&fclid=34968b6c-dff0-6323-24e1-997bde5c6257&psq=Wind+tunnel+jenis+ini+dapat+menghasilkan+kecepat

[15] N. A. P. Chory, Institut Teknologi Sepuluh Nopember, 2016. Analisa Pengaruh Variasi Sudut Y-Piece Terhadap Aliran Pada Pump Header Di Plant. vol. 4, no. August, pp. 30–59. Surabaya, Indonesia.

[16] S. E. David F. Anderson, 2001 Understanding Flight. United States of America: McGraw-Hill Companies. Available: doi: 10.1036/0071386661.

[17] D. L. Fay, 1967. BAB 2 Ansys Fluent Aliran Fluida Angew. Chemie Int. Ed. 6 (11), 951–952., pp. 4–27.

[18] M. Mulyadi, Gunadarma University. Analisis Aerodinamika Pada Sayap Pesawat Terbang Dengan Menggunakan Software Berbasis Computational Fluid Dynamics (CFD).

[19] A. T. E. Kurniawan, D. Chrismanto, and G. Rindo, 2017. Analisa Perbandingan Penggunaan Energy Saving Device (ESD). J. Tek. Perkapalan, vol. 05, no. 1, pp. 88–96.

[20] P. Iswandi, 2014. Motor AC Satu Phase dan Tiga Phase. Academia.Edu. Available:https://www.academia.edu/29519039/Motor_AC_Satu_Phase_dan_Tiga_Phase